Figure S1. Ground truth annotation workflow for mitochondria

(A) Example to illustrate the sequential steps used with Ilastik Carving module to generate the ground truth annotation for a mitochondrion in Cell 1 HEK293A prepared by chemical fixation and visualized with ~ 5 nm isotropic resolution**.** Coarse annotations for background (yellow) and object (blue) drawn in broadly spaced consecutive planes of the stack were used to seed the Ilastik Carving module from which a binary mask spaced along adjacent planes spaced 5 nm in the z-stack and corresponding to the mitochondria ground annotation was generated (magenta). Manual corrections using VAST are used as needed, to remove incorrectly assigned pixels, in this example corresponding to an adjacent ER (white arrow).

(B) Volume rendering corresponding to the ground truth annotation of the mitochondrion shown in **(A)**. Scale bar, 500 nm.

Figure S2. Ground truth annotation workflow for ER and Golgi apparatus

(A, B) Example of graph-cut assisted segmentation used to generate the ground truth annotation for ER **(A)** or mitochondria **(B)** in Cell 1 HEK293A prepared by chemical fixation and visualized with ~ 5 nm isotropic resolution**.** Coarse annotations for background (lines, solid areas in pink) and object (dotted lines in yellow) drawn in the indicated broadly spaced planes of the stack were used as seeds to obtain the ground truth annotations spaced 5 nm apart generated by the graph-cut assisted segmentation program.

Figure S3. **3D-Unet architecture**

Schematic representation of the steps used to train the 3D U-net encoder-decoder neural network. The input for the neural network mode are 3D blocks consisting of a stack of consecutive FIB-SEM images (size 204 x 204 x 204 voxels). The 3D block is subjected to consecutive 3 x 3 x 3 convolutions without padding (purple) and down sampling operators with 2 x 2x 2 max-pooling (pink), followed by consecutive up sampling by a factor of 2 (yellow) of the feature maps. During up sampling, the feature maps are concatenated with previous feature maps from the down sampling branch that had been exposed to central cropping; this step also includes consecutive 3 x 3 x 3 convolutions without padding (purple). The output of the neural network model is a feature map (size 110 x 110 x 110 voxels) of two channels, representing the foreground (FG) and background (BG = 1- FG) probability maps, respectively. Number of featured maps are denoted in red, spatial dimensions at the indicated steps in the neural network, in black. Figure designed based on PlotNeuralNet (https://github.com/HarisIqbal88/PlotNeuralNet) (adapted from (Sheridan et al., 2022).

Figure S4. Examples of network behavior during training

(A-C) Examples of plots of cross entropy loss used to evaluate the predicting behavior of the indicated neural network models for **(A)** Mitochondria, **(B)** Golgi or **(C)** ER obtained during training using FIB-SEM volume data of cells prepared by chemical fixation obtained at ~ 5 nm resolution. Cross entropy values were obtained using ground truth annotations from the training set or from naïve cells not used during training, respectively. The gray area shows the first appearance of relatively stable cross-entropy loss and absence of major spikes obtained by the models during 20,000 consecutive training iterations; these models were then used to evaluate their network architecture and prediction performance.

Figure S5. Use of CLAHE to equalize the contrast of FIB-SEM images

(A-D) Single plane views of FIB-SEM volume data after contrast equalization using CLAHE with a clip limit of 0.02. The samples were prepared by CF **(A, B)** or HFFS **(C, D)** and imaged at ~ 5 nm isotropic resolution.

Figure S6. Comparison of metrics used to validate the prediction accuracy of neural models predicting mitochondria, ER and Golgi apparatus

Ground truth annotations from FIB-SEM volume data from the indicated cells at ~ 5 nm isotropic resolution prepared by CF or HPFS were used for training to generate models for mitochondria, ER and Golgi apparatus. The histogram plots show F1, precision and recall metrics obtained using ground truth annotations not used for training. The results also show metrics obtained after fine-tunning with a small number of additional training iterations using ground truth annotations from the naïve cell. Details of datasets, ground-truth annotations and models are summarized in Tables S4, S5 and S2.

Figure S7. Steps to determine the diameter of the nuclear pore membrane

(A) Nuclear pore predictions for all the pores on the nuclear envelope of naïve interphase cell 19 (Hela-2) prepared by HPFS and visualized at 4 x 4 x 5.3 nm isotropic resolution. The nuclear pore predictions were obtained using model 1986 trained without fine tuning with ground truths annotations for Cell 13 (Hela) prepared by HPFS and imaged at ~ 5 nm isotropic resolution.

(B) Volume location of the centroid of each of the predicted nuclear pore's color coded according to their relative position along the Z-axis (top panel) and surface rendition of the nuclear envelope

(green) obtain by alpha-shape triangulation of the centroids (see Methods). Orthonormal vectors associated with each triangle are shown (red).

(C) Example of realignment of a nuclear pore from its acquisition orientation in the FIB-SEM volume image to a new view with the nuclear envelope orthogonal to the Z-axis; side views and volume rendition of the nuclear pore prediction are shown.

(D) Single plane on face and orthogonal views of a nuclear pore centered on the middle of the nuclear envelope (left panels) and examples of the intensity plots used to estimate the membrane pore diameters by determining the distance separating the two intensity minima along the indicated axis (right panels). The nuclear pore diameter is reported as the average of 10 values obtained 18 ° apart (inset in left panel).

(E) Three-dimensional distribution of nuclear pores on the nuclear envelopes of Cells 15 and 17 color coded by a heat map as a function of membrane pore diameter.

Figure S8. Definition of metrics used to characterize clathrin coated structures.

(A) Schematic representation of the timeline to describe the formation of a clathrin coated pit mediated by the assembly of the clathrin coat (Kirchhausen et al., 2014). The last step mediated by fission of the membrane neck connecting the mature coated pit from the originating membrane results in formation of the fully formed coated vesicle. Metrics of neck width, pit height, full width at half maximum and major and minor axis of the fitted ellipse used to morphologically describe the clathrin coated pits are shown.

(B) Metrics used to characterize clathrin coated vesicles.

(C) Example of a single plane from a selected endocytic clathrin coated pit in a cell prepared by HPFS and imaged by FIB-SEM at ~ 5 nm isotropic resolution. The darker voxels corresponding to the deformed membrane and the coat surrounding the pit (left panel) were segmented using an Otsu-based intensity threshold approach (Otsu, 1979) to generate a skeletonized binary mask (central panel) which was then used to fit the ellipse (right panel).

Figure S9. Identification of clathrin coated pits, coated vesicle.

Data shown in this figure for Cells 12, 13, 17 and 17 were generated using the coated pit model employed in Fig 7 obtained by training with ground truth annotations from Cell 12 prepared by HPFS and imaged at ~ 5 nm isotropic resolution.

(**A**) Violin plots of major and minor axis and eccentricity of the fitted ellipse of all pits and vesicles in the raw images of the structures identified by the coated pit model.

(B) Scatter plot of height versus neck width of endocytic clathrin coated pits clustered in two groups associated with early and late stages of pit formation (left panel). The histogram compares height and major axis for the fitted ellipse of late endocytic coated pits and coated vesicles, respectively.
(C) Scatter plot of height versus neck width of 'secretory' clathrin coated pits associated with internal membranes.

Figure S10. F1 as a metric to compare ground truth annotations with model predictions
Ground truth annotations consist of true positive (TP) and false negatives (FN) voxels and define presence or absence of a perfect match with the subcellular structure of interest. The model predicts voxels with true (TP) and false positives (FP) values, depending on whether it considers them as representing or not the structure of interest. F1, as defined in the figure, is used as a practical metric to evaluate the prediction accuracy of the neural network to identify the structure of interest. A perfect model prediction would yield F1=1 with FP=0, FN=0.

References

Chou, Y.-Y., Upadhyayula, S., Houser, J., He, K., Skillern, W., Scanavachi, G., Dang, S., Sanyal, A., Ohashi, K.G., Caprio, G.D., et al. (2021). Inherited nuclear pore substructures template post-mitotic pore assembly. Developmental Cell.

Kirchhausen, T., Owen, D., and Harrison, S.C. (2014). Molecular structure, function, and dynamics of clathrin-mediated membrane traffic. Cold Spring Harbor Perspectives in Biology *6*, a016725.

Otsu, N. (1979). A Threshold Selection Method from Gray-Level Histograms. Ieee Transactions Syst Man Cybern *9*, 62–66.

Sheridan, A., Nguyen, T., Deb, D., Lee, W.-C.A., Saalfeld, S., Turaga, S., Manor, U., and Funke, J. (2022). Local Shape Descriptors for Neuron Segmentation. Biorxiv 2021.01.18.427039.

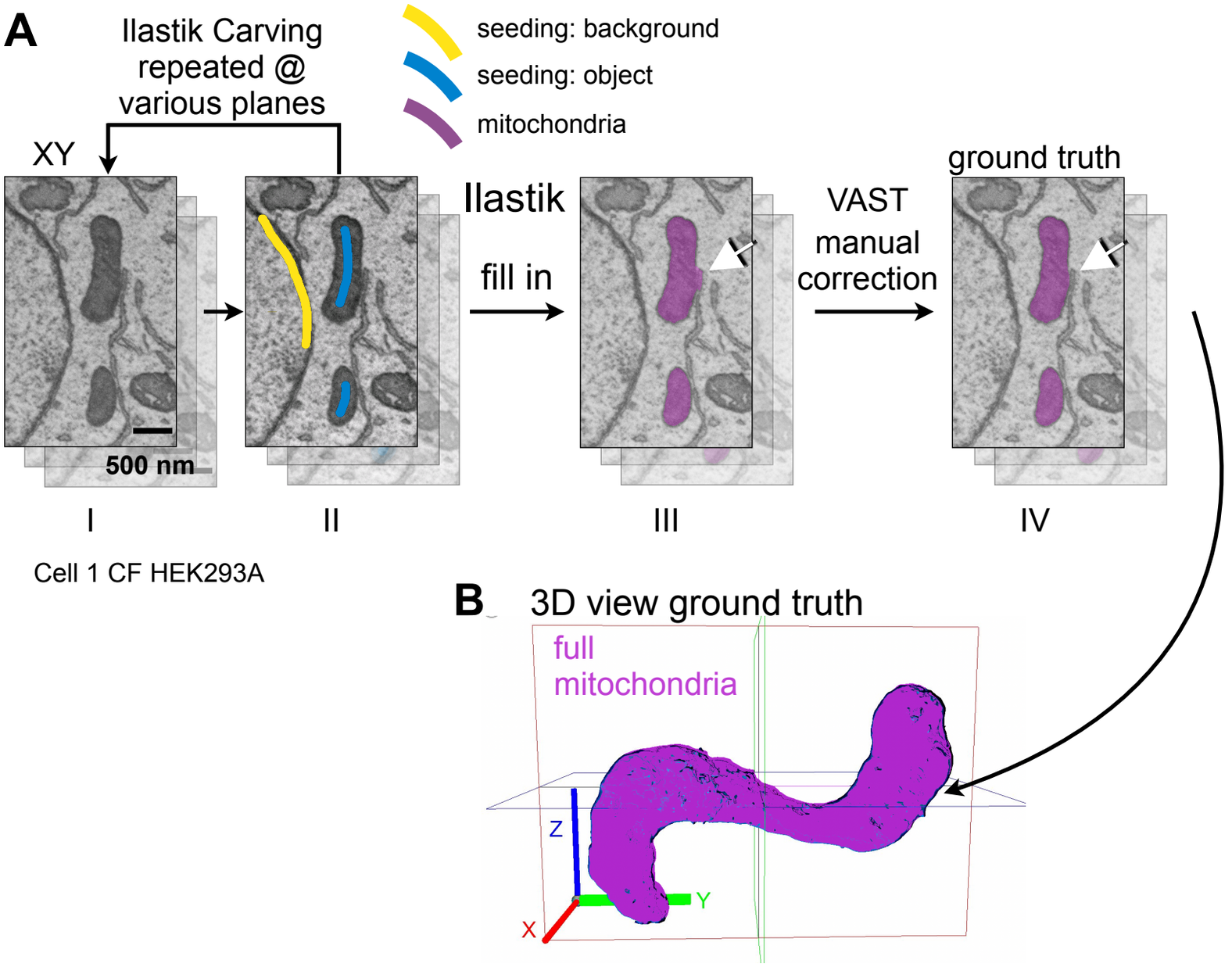
A
Ilastik Carving
repeated @
various planes
XY
seeding: background
seeding: object
mitochondria
Ilastik
fill in
VAST
manual
correction
ground truth
500 nm
I
II
III
IV
Cell 1 CF HEK293A
B
3D view ground truth
full
mitochondria
Z
Y
X

Figure S1

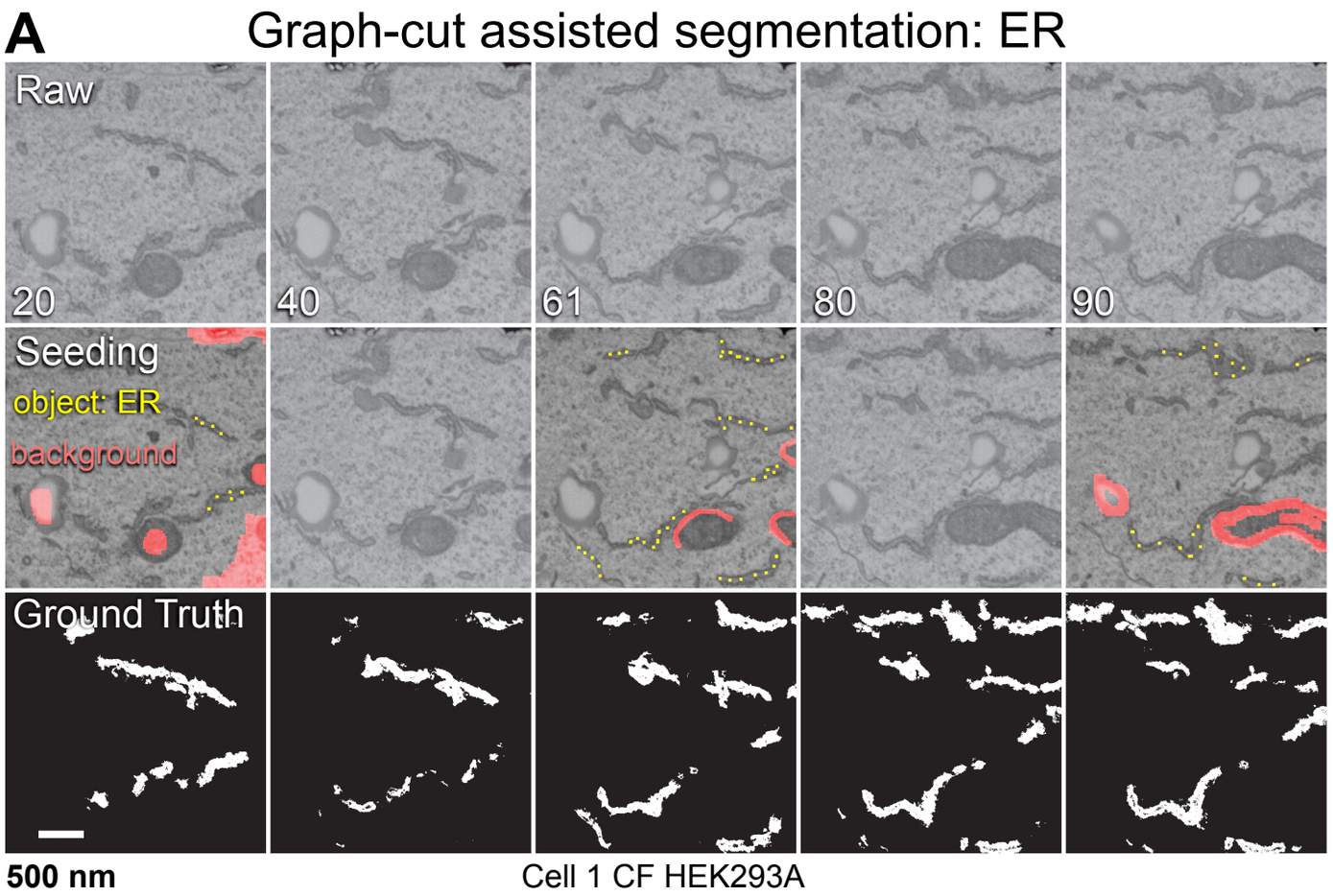
A
Graph-cut assisted segmentation: ER
Raw
20
40
61
80
90
Seeding
object: ER
background
Ground Truth
500 nm
Cell 1 CF HEK293A
B
Graph-cut assisted segmentation: Golgi apparatus
Raw
206
215
229
235
241
Seeding
object: Golgi
background
Ground Truth
500 nm
Cell 1 CF HEK293A

Figure S2

3D U-net: 3D convolutional neural network

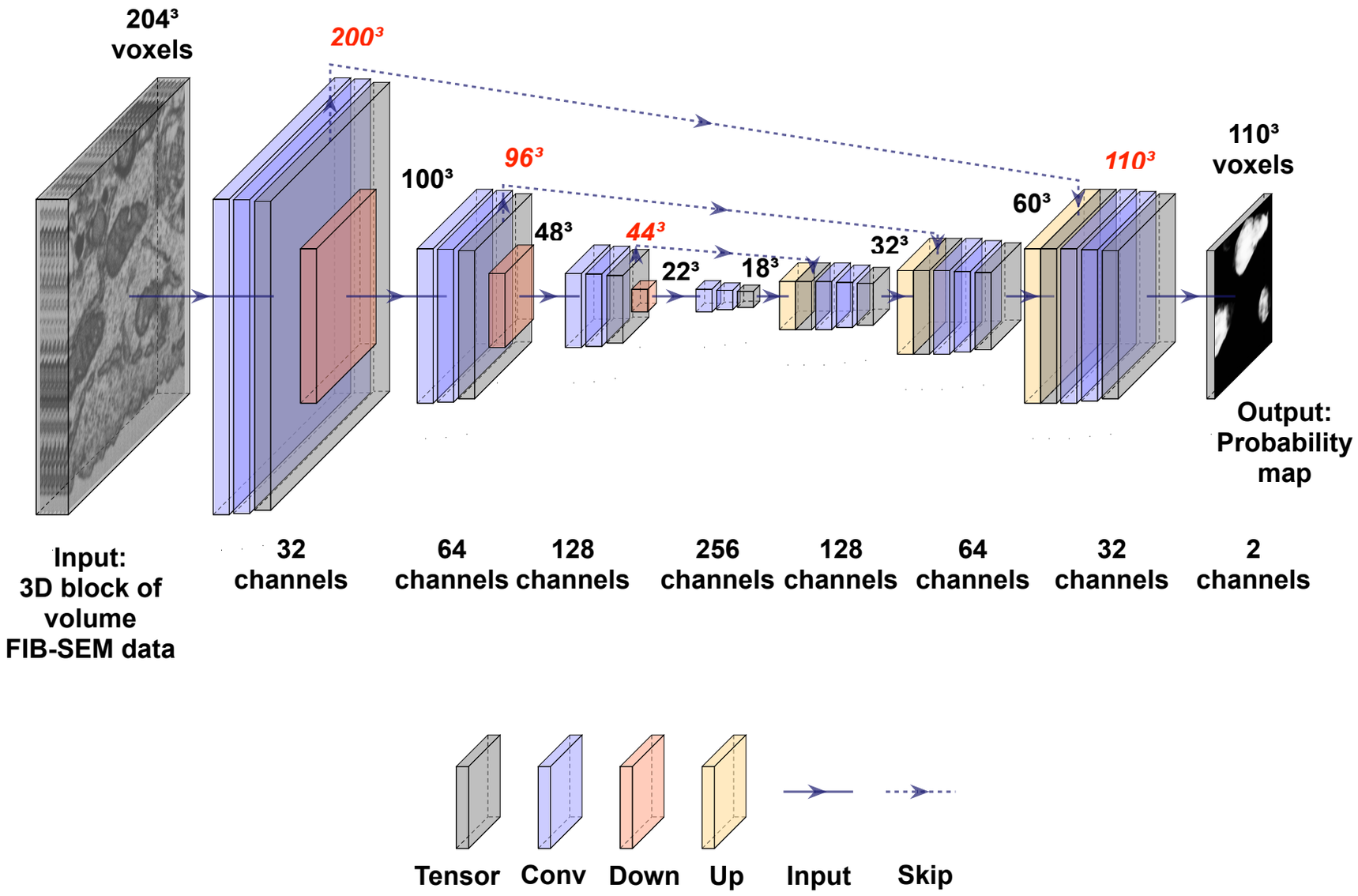

Figure S3

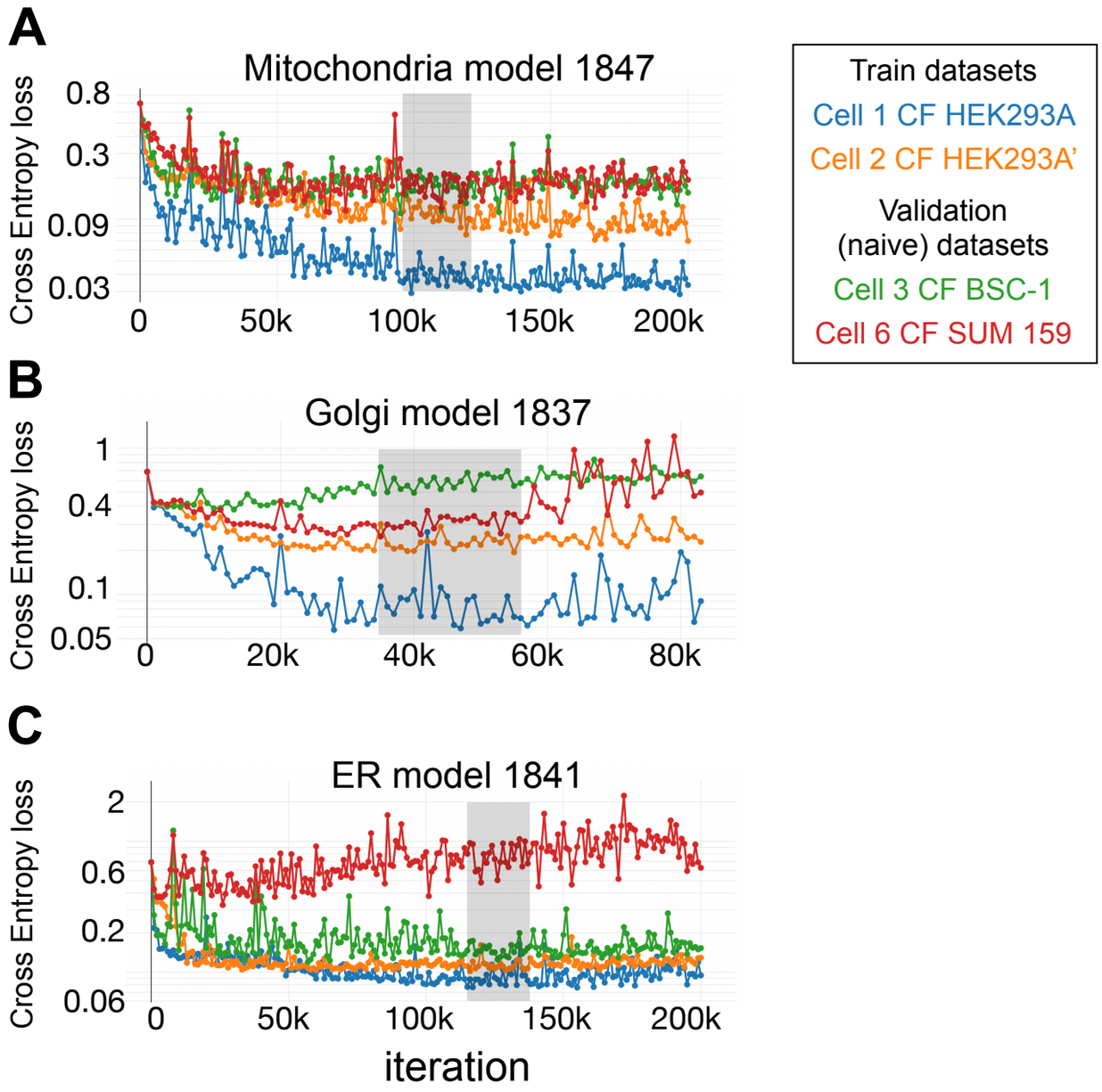
A
Mitochondria model 1847
Cross Entropy loss
0.8
0.3
0.09
0.03
0
50k
100k
150k
200k
B
Golgi model 1837
Cross Entropy loss
1
0.4
0.1
0.05
0
20k
40k
60k
80k
C
ER model 1841
Cross Entropy loss
2
0.6
0.2
0.06
0
50k
100k
150k
200k
iteration
Train datasets
Cell 1 CF HEK293A
Cell 2 CF HEK293A'
Validation
(naive) datasets
Cell 3 CF BSC-1
Cell 6 CF SUM 159

Figure S4

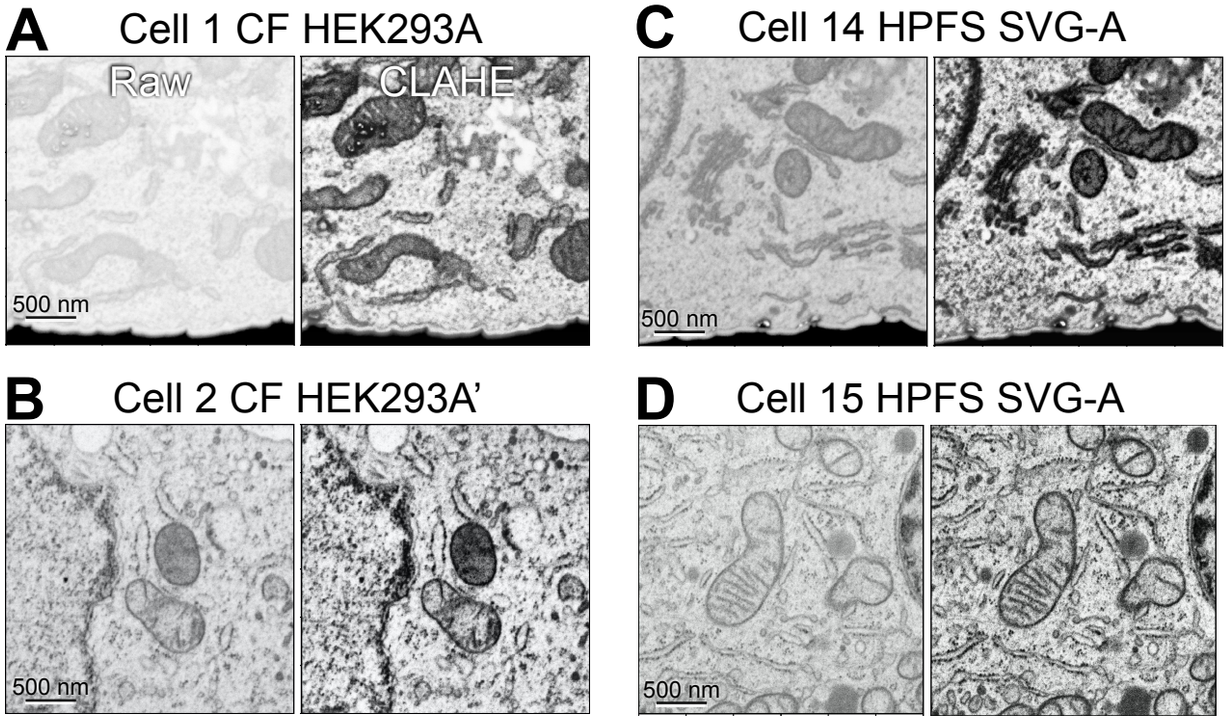
A
Cell 1 CF HEK293A
Raw
CLAHE
500 nm
B
Cell 2 CF HEK293A'
500 nm
C
Cell 14 HPFS SVG-A
500 nm
D
Cell 15 HPFS SVG-A
500 nm

Figure S5

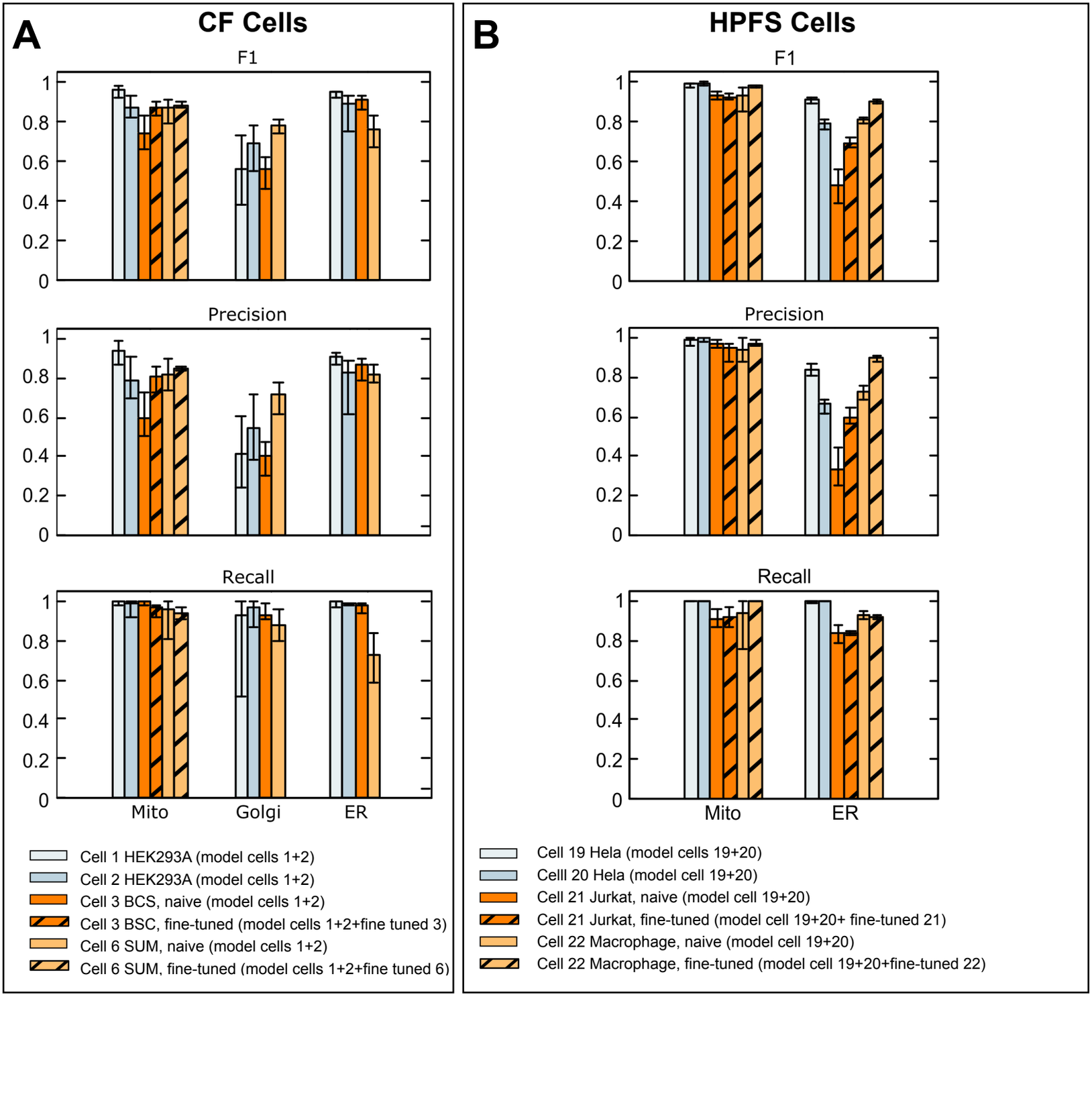
A
CF Cells
F1
Precision
Recall
0
0.2
0.4
0.6
0.8
1
Mito
Golgi
ER
Cell 1 HEK293A (model cells 1+2)
Cell 2 HEK293A (model cells 1+2)
Cell 3 BCS, naive (model cells 1+2)
Cell 3 BSC, fine-tuned (model cells 1+2+fine tuned 3)
Cell 6 SUM, naive (model cells 1+2)
Cell 6 SUM, fine-tuned (model cells 1+2+fine tuned 6)
B
HPFS Cells
F1
Precision
Recall
Mito
ER
Cell 19 Hela (model cells 19+20)
Celll 20 Hela (model cell 19+20)
Cell 21 Jurkat, naive (model cell 19+20)
Cell 21 Jurkat, fine-tuned (model cell 19+20+ fine-tuned 21)
Cell 22 Macrophage, naive (model cell 19+20)
Cell 22 Macrophage, fine-tuned (model cell 19+20+fine-tuned 22)

\

Figure S6

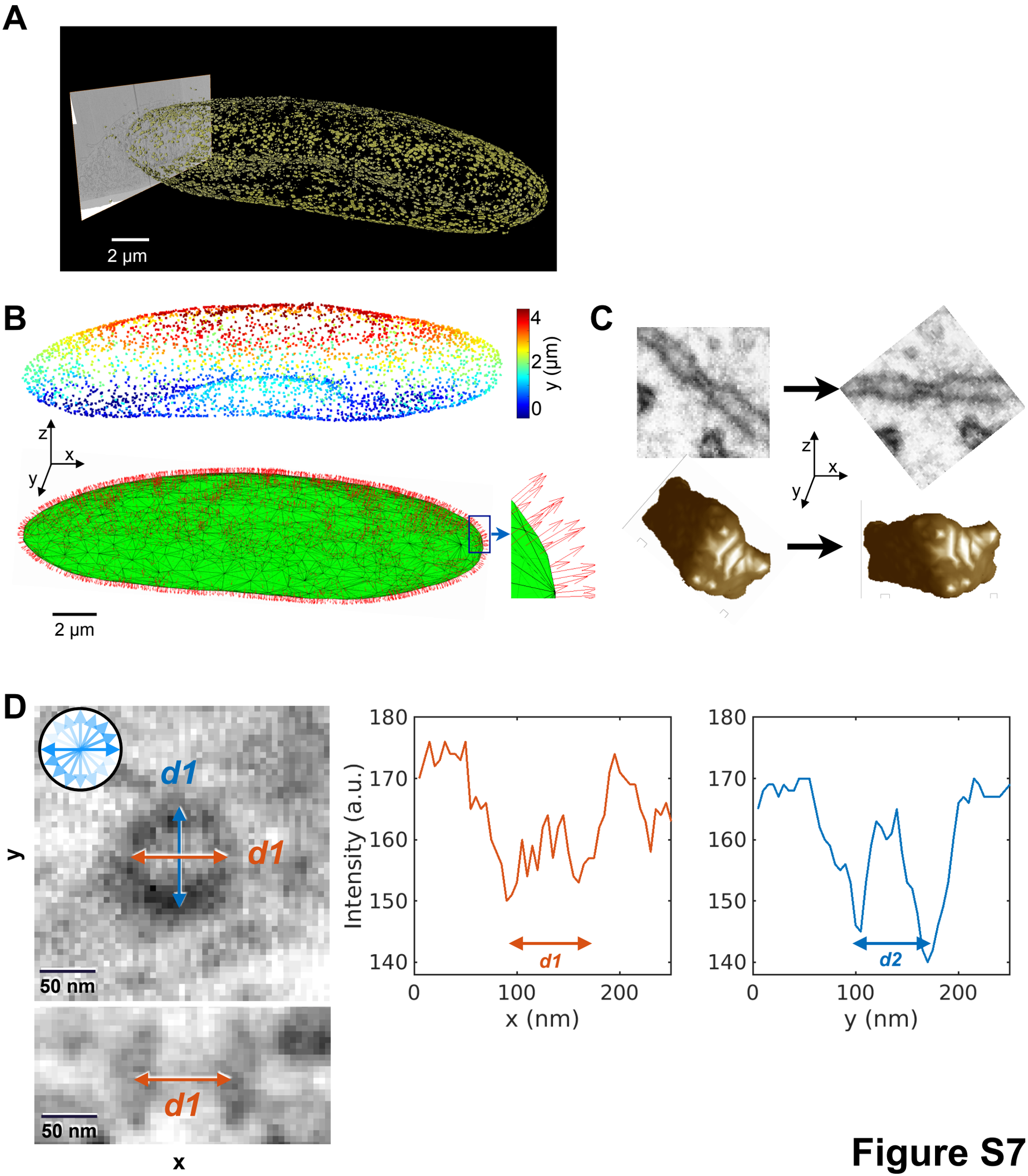
A
2 µm
B
4
2
0
y (µm)
z
x
y
2 µm
C
z
x
y
D
d1
d1
50 nm
d1
50 nm
y
x
Intensity (a.u.)
180
170
160
150
140
0
100
200
x (nm)
d1
180
170
160
150
140
0
100
200
y (nm)
d2

Figure S7

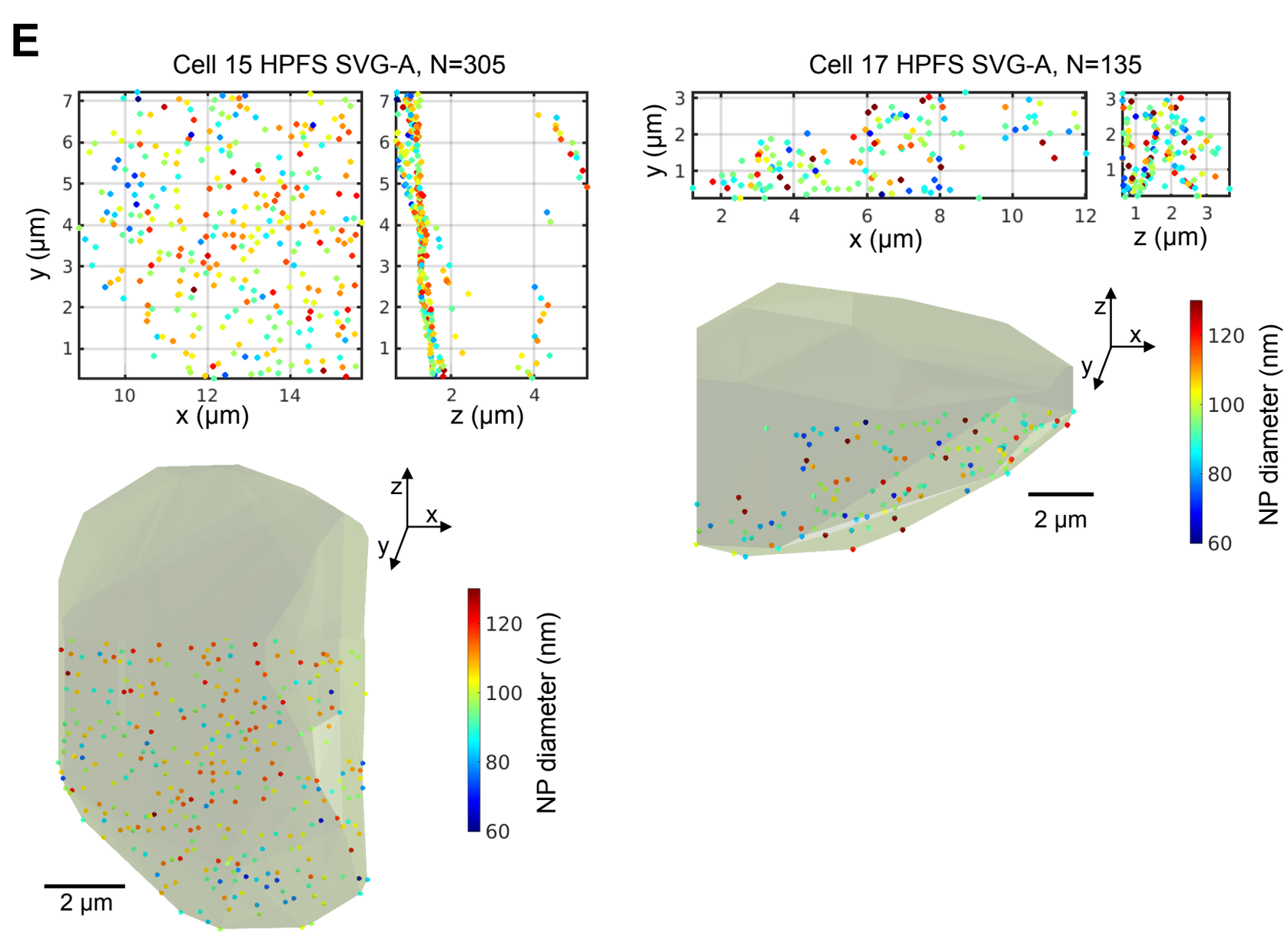
E
Cell 15 HPFS SVG-A, N=305
y (µm)
x (µm)
z (µm)
Cell 17 HPFS SVG-A, N=135
y (µm)
x (µm)
z (µm)
z
x
y
2 µm
NP diameter (nm)
120
100
80
60

Figure S7

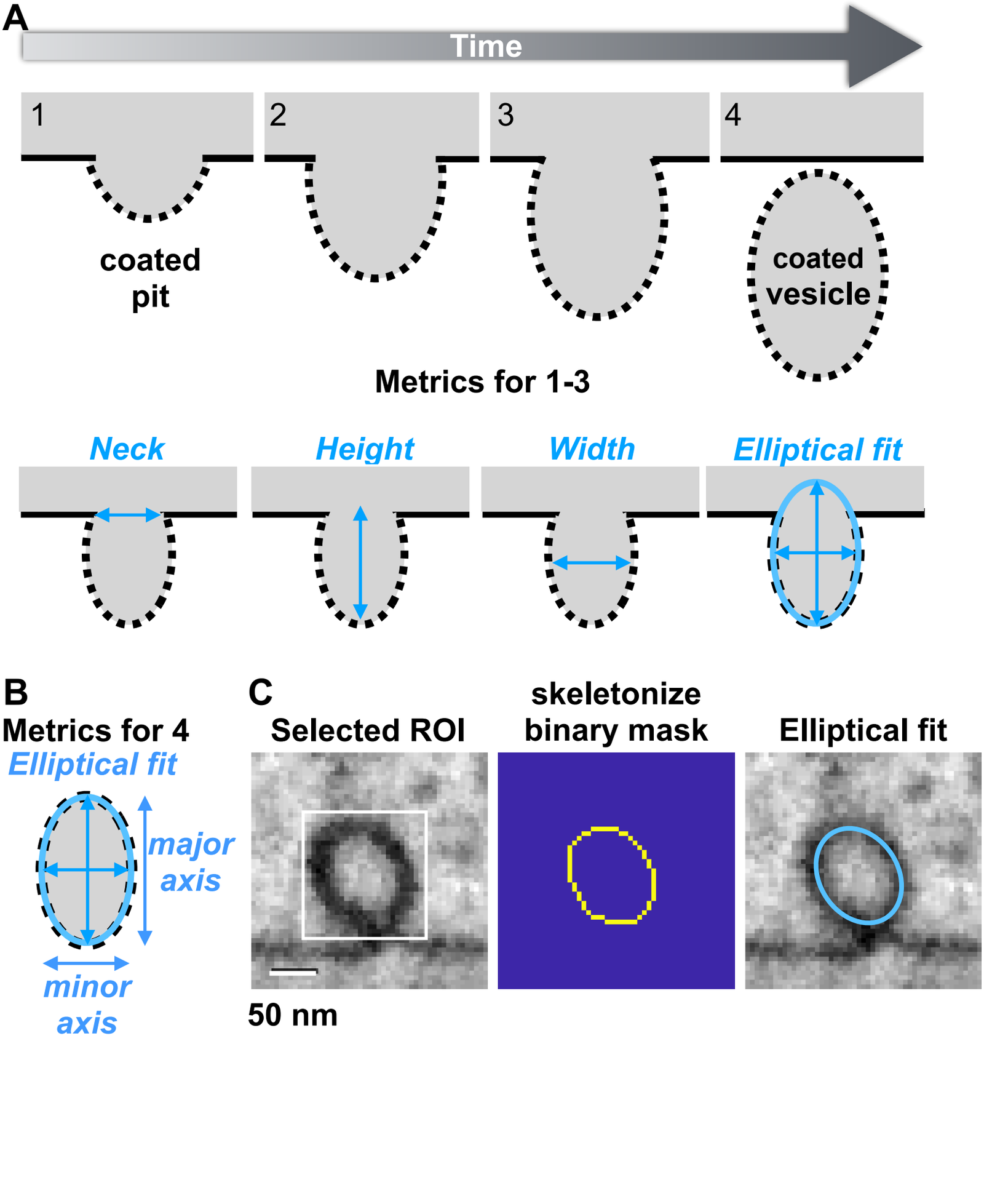
A
Time
1
2
3
4
coated pit
coated vesicle
Metrics for 1-3
Neck
Height
Width
Elliptical fit
B
Metrics for 4
Elliptical fit
major axis
minor axis
C
Selected ROI
skeletonize binary mask
Elliptical fit
50 nm

Figure S8

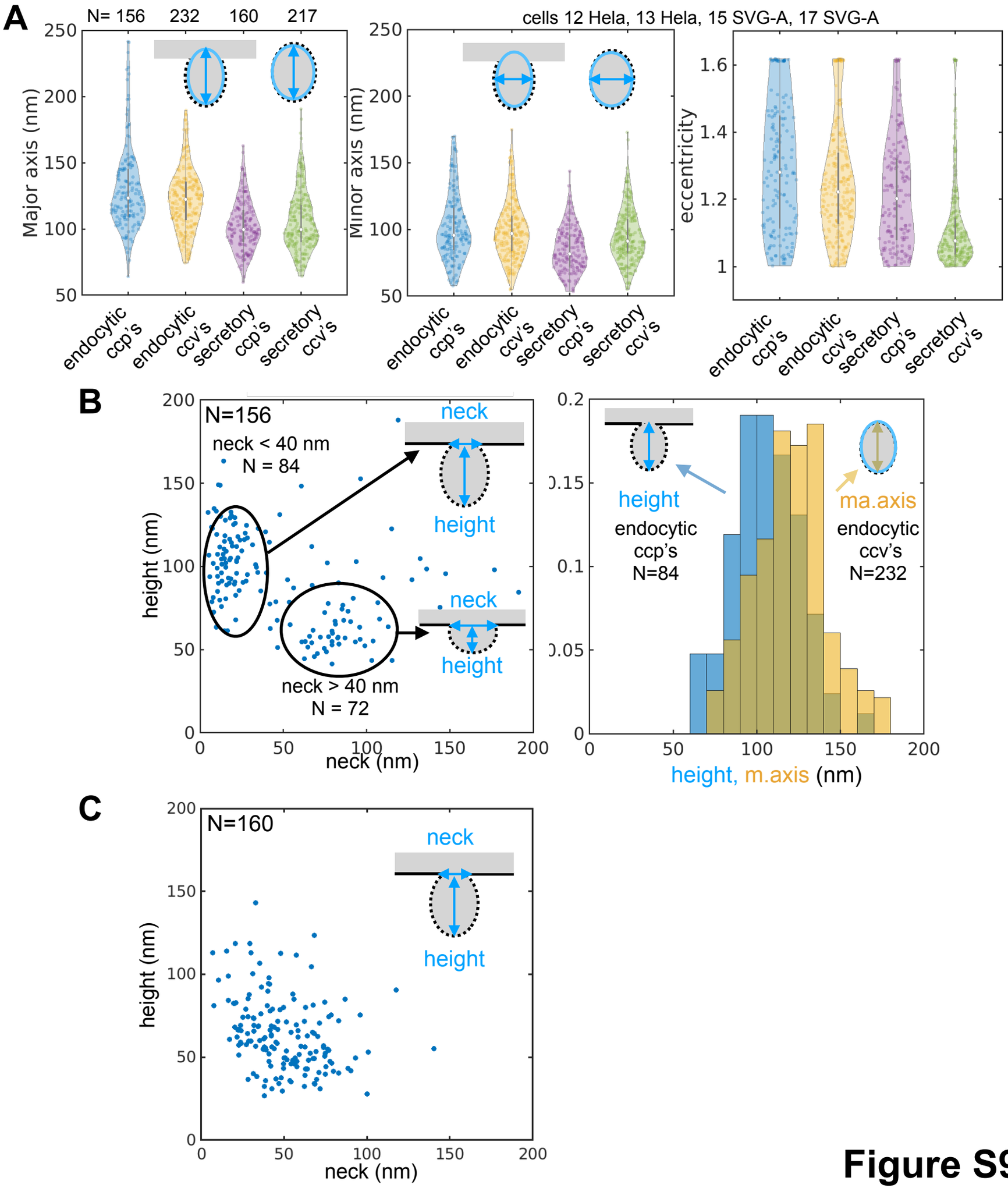
A
N= 156 232 160 217
cells 12 Hela, 13 Hela, 15 SVG-A, 17 SVG-A
Major axis (nm)
Minor axis (nm)
eccentricity
endocytic ccp's
endocytic ccv's
secretory ccp's
secretory ccv's
B
N=156
neck < 40 nm
N = 84
neck > 40 nm
N = 72
neck
height
height (nm)
neck (nm)
height
endocytic ccp's N=84
ma.axis
endocytic ccv's N=232
height, m.axis (nm)
C
N=160
neck
height
height (nm)
neck (nm)

Figure S9

definition of metrics

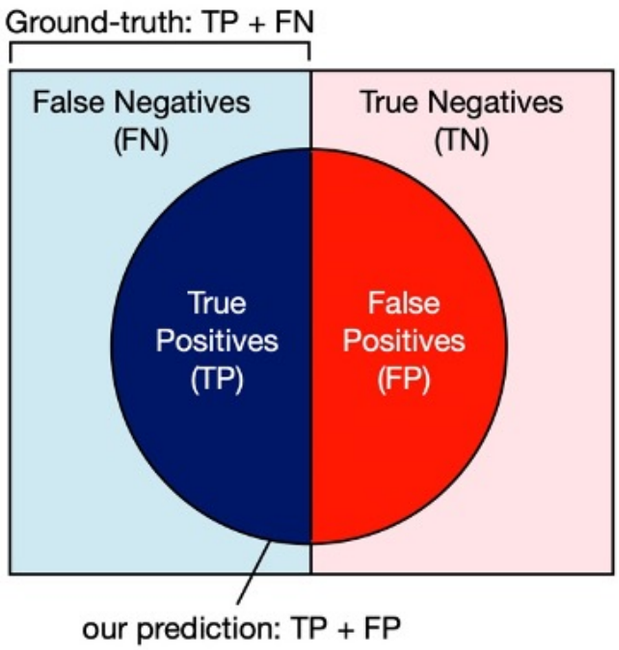

$$F1 = \frac{TP}{TP + (FP + FN) / 2}$$

Figure S10

Table S1. Cells used in this study

Cell 1, 1a

Description: HEK293A human epithelial derived cell stably expressing eGFP-connexin43 (ATCC, crl-1573)
Protocol: Chemical fixation
Contributions: Sample provided by Teresa Rodrigues and Henrique Girão (Universidade de Coimbra), prepared for imaging by Giovanni de Nola and Teresa Rodrigues; imaging and pre-processing by Tegy John Vadakkan; post-processing by Ben Gallusser
Publication: this study
Voxel size: 5 nm x 5 nm x 5 nm

Cell 2

Description: HEK293A human epithelial derived cell stably expressing eGFP-connexin43 (ATCC, crl-1573)
Protocol: Chemical fixation
Contributions: Sample provided by Teresa Rodrigues and Henrique Girão (Universidade de Coimbra), prepared for imaging by Giovanni de Nola and Teresa Rodrigues; imaging and pre-processing by Tegy John Vadakkan; post-processing by Ben Gallusser
Publication: this study
Voxel size: 5 nm x 5 nm x 5 nm

Cell 3

Description: BSC-1 African green monkey kidney epithelial derived cells stably expressing Lamp1-eGFP and mCherry-Galectin3
Protocol: Chemical fixation
Contributions: Sample prepared by Teresa Rodrigues (Universidade de Coimbra), prepared for imaging by Giovanni de Nola and Teresa Rodrigues; imaging and pre-processing by Tegy John Vadakkan; post-processing by Ben Gallusser
Publication: this study
Voxel size: 5 nm x 5 nm x 5 nm

Cell 4

Description: BSC-1 African green monkey kidney epithelial derived cells stably expressing Lamp1-eGFP and mCherry-Galectin3
Protocol: Chemical fixation
Contributions: Sample prepared by Teresa Rodrigues, prepared for imaging by Giovanni de Nola and Teresa Rodrigues; imaging and pre-processing by Tegy John Vadakkan; post-processing by Ben Gallusser
Publication: this study
Voxel size: 5 nm x 5 nm x 5 nm

Cell 5

Description: SVG-A human fetal glial derived cells
Protocol: Chemical fixation
Contributions: Prepared for imaging by Rasmus Herlo and Max Paget; imaging and pre-processing by Tegy John Vadakkan; post-processing by Ben Gallusser
Publication: (Chou et al., 2021)
Voxel size: 5 nm x 5 nm x 5 nm

Cell 6, 6a

Description: interphase SUM159 human breast carcinoma derived cell gene edited to express eGFP-Nup133
Protocol: Chemical fixation
Contributions: Prepared for imaging by Justin Houser; imaging and pre-processing by Tegy John Vadakkan; post-processing by Ben Gallusser
Publication: (Chou et al., 2021)
Voxel size: 5 nm x 5 nm x 5 nm

Cell 7

Description: mitotic SUM159 human breast carcinoma derived cell gene edited to express eGFP-Nup133
Protocol: Chemical fixation
Contributions: Prepared for imaging by Justin Houser; imaging and pre-processing by Tegy John Vadakkan; post-processing by Ben Gallusser
Publication: (Chou et al., 2021)
Voxel size: 5 nm x 5 nm x 5 nm

Cell 8

Description: pro-metaphase SUM159 human breast carcinoma derived cell gene edited to express eGFP-Nup133
Protocol: Chemical fixation
Contributions: Prepared for imaging by Justin Houser; imaging and pre-processing by Justin Houser; post-processing by Ben Gallusser
Publication: (Chou et al., 2021)
Voxel size: 10 nm x 10 nm x 10 nm

Cell 9
Description: interphase SUM159 human breast carcinoma derived cell gene edited to express eGFP-Nup133
Protocol: Chemical fixation
Contributions: Prepared for imaging by Justin Houser; imaging and pre-processing by Justin Houser; post-processing by Ben Gallusser
Publication: (Chou et al., 2021)
Voxel size: 10 nm x 10 nm x 10 nm

Cell 11
Description: interphase U2OS human sarcoma derived cell
Protocol: HPFS
Contributions: Prepared for imaging by Gleb Shtengel (HHMI/Janelia) and C. Shan Xu (HHMI/Janelia); post-processing by Ben Gallusser
Publication: this study
Voxel size: 8 nm x 8 nm x 8 nm

Cell 12
Description: HeLa cell
Protocol: HPFS
Contributions: Sample provided and prepared for imaging by HHMI/Janelia; imaging and pre-processing by Tegy John Vadakkan
Publication: this study
Voxel size: 5 nm x 5 nm x 5 nm

Cell 13
Description: HeLa cell
Protocol: HPFS
Contributions: Sample provided and prepared for imaging by HHMI/Janelia; imaging and pre-processing by Tegy John Vadakkan
Publication: this study
Voxel size: 5 nm x 5 nm x 5 nm

Cell 13a
Description: SVG-A human fetal glial derived cells stably expressing mCherry-Galectin8
Protocol: HPFS
Contributions: Prepared for imaging by Anwesha Sanyal and Elliott Somerville; imaging and pre-processing by Tegy John Vadakkan
Publication: this study
Voxel size: 5 nm x 5 nm x 5 nm

Cell 15
Description: SVG-A human fetal glial derived cells stably expressing mCherry-Galectin8
Protocol: HPFS
Contributions: Sample provided by Anwesha Sanyal, prepared for imaging by Anwesha Sanyal and Elliott Somerville; imaging and pre-processing by Tegy John Vadakkan
Publication: this study
Voxel size: 5 nm x 5 nm x 5 nm

Cell 16
Description: SVG-A human fetal glial derived cells stably expressing mCherry-Galectin8
Protocol: HPFS
Contributions: Sample provided by Anwesha Sanyal, prepared for imaging by Anwesha Sanyal and Elliott Somerville; imaging and pre-processing by Tegy John Vadakkan
Publication: this study
Voxel size: 5 nm x 5 nm x 5 nm

Cell 17
Description: SVG-A human fetal glial derived cells stably expressing mCherry-Galectin8
Protocol: HPFS
Contributions: Sample provided by Anwesha Sanyal, prepared for imaging by Anwesha Sanyal and Elliott Somerville; imaging and pre-processing by Tegy John Vadakkan
Publication: this study
Voxel size: 5 nm x 5 nm x 5 nm

Cell 19
Description: Hela-2 Wild-type, interphase HeLa cell (ATCC CCL-2)
Protocol: HPFS
Contributions: Sample provided by Aubrey Weigel (HHMI/Janelia), prepared for imaging by Gleb Shtengel (HHMI/Janelia), with imaging and post-processing by C. Shan Xu (HHMI/Janelia)
Publication: (Xu et al., 2021)
Voxel size: 4 nm x 4 nm x 5.2 nm

Cell 20
Description: Hela-3 Wild-type, interphase HeLa cell (ATCC CCL-2)
Protocol: HPFS
Contributions: Sample provided by Aubrey Weigel (HHMI/Janelia), prepared for imaging by Gleb Shtengel (HHMI/Janelia), with imaging and post-processing by C. Shan Xu (HHMI/Janelia)
Publication: (Xu et al., 2021)
Voxel size: 4 nm x 4 nm x 3.2 nm

Cell 21
Description: Jurkat-1 Wild-type, Clone E6-1 (ATCC TIB-152)
Protocol: HPFS
Contributions: Sample provided by Huxley Hoffman and Schuyler van Engelenburg (U. Denver), prepared for imaging by Gleb Shtengel (HHMI/Janelia), with imaging and post-processing by C. Shan Xu (HHMI/Janelia).
Publication: (Xu et al., 2021)
Voxel size: 4 nm x 4 nm x 3.4 nm

Cell 22
Description: Macrophage-2, Wild-type THP-1 macrophage. THP-1 human monocyte cell line (ATC TIB-202) treated with PMA to differentiate into macrophages.
Protocol: HPFS
Contributions: Sample provided by Aubrey Weigel (HHMI/Janelia), prepared for imaging by Gleb Shtengel (HHMI/Janelia), with imaging and post-processing by C. Shan Xu (HHMI/Janelia)
Publication: (Xu et al., 2021)
Voxel size: 4 nm x 4 nm x 3.4 nm

Description for each sample includes cell type, fixation protocol (CF or HPFS), source and FIB-SEM resolution**.**

Supplementary References

Chou, Y.-Y., Krupp, A., Kaynor, C., Gaudin, R., Ma, M., Cahir-McFarland, E., and Kirchhausen, T. (2016a). Inhibition of JCPyV infection mediated by targeted viral genome editing using CRISPR/Cas9. Scientific Reports *6*, 36921.

Chou, Y.-Y., Cuevas, C., Carocci, M., Stubbs, S.H., Ma, M., Cureton, D.K., Chao, L., Evesson, F., He, K., Yang, P.L., et al. (2016b). Identification and characterization of a novel broad spectrum virus entry inhibitor. J Virol *90*, 4494–4510.

Chou, Y.-Y., Upadhyayula, S., Houser, J., He, K., Skillern, W., Scanavachi, G., Dang, S., Sanyal, A., Ohashi, K.G., Caprio, G.D., et al. (2021). Inherited nuclear pore substructures template post-mitotic pore assembly. Developmental Cell.

Ehrlich, M., Boll, W., Oijen, A. van, Hariharan, R., Chandran, K., Nibert, M.L., and Kirchhausen, T. (2004). Endocytosis by random initiation and stabilization of clathrin-coated pits. Cell *118*, 591–605.

Xu, C.S., Pang, S., Shtengel, G., Müller, A., Ritter, A.T., Hoffman, H.K., Takemura, S., Lu, Z., Pasolli, H.A., Iyer, N., et al. (2021). An open-access volume electron microscopy atlas of whole cells and tissues. Nature *599*, 147–151.

Table S2. Size of hold out volumes containing ground truths and their use for model training, validation and prediction

Cell	Cell type	Laboratory	Fixation Protocol	Voxel size nm (x, y, z)	Use
1	HEK293A interphase	this study	CF	5 x 5 x 5	training, validation
2	HEK293A interphase	this study	CF	5 x 5 x 5	training, validation
3	BSC-1 interphase	this study	CF	5 x 5 x 5	validation
6	SUM 159 interphase	this study	CF	5 x 5 x 5	validation
8	SUM 159 prometaphase	this study	CF	10 x 10 x 10	prediction
9	SUM 159 interphase	this study	CF	10 x 10 x 10	prediction
12	HeLa interphase	this study	HPFS	5 x 5 x 5	training, prediction
13	HeLa interphase	this study	HPFS	5 x 5 x 5	training, prediction
13a	SVG-A interphase	this study	HPFS	5 x 5 x 5	training, prediction
15	SVG-A interphase	this study	HPFS	5 x 5 x 5	prediction
16	SVGA interphase	this study	HPFS	5 x 5 x 5	prediction
17	SVG-A interphase	this study	HPFS	5 x 5 x 5	prediction
19	HeLa-2 interphase	COSEM HHMI/Janelia	HPFS	4 x 4 x 5.2	training, validation
20	HeLa-3 interphase	COSEM HHMI/Janelia	HPFS	4 x 4 x 3.2	training, validation
21	Jurkat-1 interphase	COSEM HHMI/Janelia	HPFS	4 x 4 x 3.4	validation
22	Macrophage-2 interphase	COSEM HHMI/Janelia	HPFS	4 x 4 x 3.4	validation

Description for each sample includes cell type, stage during cell cycle, fixation protocol (CF or HPFS), FIB-SEM resolution and use of the ground truths for model training, validation and prediction.

Table S3. Modes of data augmentation used in this study

Augmentation	Parameter	Value
Mirror	axes	x, y, z
Transpose	axes	x, y, z
Elastic	control point spacing	32, 32, 32
	jitter sigma	2, 2, 2
	subsample	4
Rotation	axes	x, y
Mirror	axes	x, y, z
Transpose	axes	x, y, z
Intensity	scale	in [0.85, 1.15]
	shift	in [0.85, 1,15]

Type of augmentation and parameters to modify the ground truths used during model training. Their detailed description is found in GUNPOWDER (http://funkey.science/gunpowder/api.html#augmentation-nodes). Since the rotation operation was performed in two dimensions, it was necessary to perform twice the mirror and transpose operations in order to obtain all possible orientations of the hold block containing the ground truth.

Table S4. Procedures used to generate ground truths

Cell	Structure	Method used to generate ground truth	Voxel Size (nm) (x, y, z)	Training Block Size (um^3) ROI (voxels)	Validation Block Size (um^3) ROI (voxels)
1	Mitochondria	Ilastik	5 x 5 x 5	57.8 um^3 1200 x 700 x 550	22.5 um^3 600 x 400 x 750
2	Mitochondria	Ilastik, VAST	5 x 5 x 5	80.4 um^3 650 x 900 x 1100	15.3 um^3 450 x 800 x 340
3	Mitochondria	Ilastik, VAST	5 x 5 x 5	-	35.4 um^3 700 x 540 x 750
6	Mitochondria	Ilastik, VAST	5 x 5 x 5	-	7.6 um^3 241 x 476 x 528
1	ER	GC, VAST	5 x 5 x 5	59.7 um^3 600 x 590 x 1350	11.1 um^3 600 x 590 x 250
2	ER	GC	5 x 5 x 5	14.8 um^3 500 x 395 x 600	4.6 um^3 300 x205 x 600
3	ER	GC	5 x 5 x 5	-	2.1 um^3 204 x 204 x 400
6	ER	GC, VAST	5 x 5 x 5	-	7.5 um^3 241 x 476 x 528
1	Golgi	GC	5 x 5 x 5	47.1 um^3 469 x 650 x 510 400 x 400 x 875 350 x 400 x 400 230 x 250 x 440	105 um^3 5250 x 400 x 400
2	Golgi	GC	5 x 5 x 5	9.4 um^3 300 x 500 x 500	5.2 um^3 230 x 400 x 450
3	Golgi	GC, VAST	5 x 5 x 5	-	2.8 um^3 210 x 283 x 371
6	Golgi	GC, VAST	5 x 5 x 5	-	3.1 um^3 284 x 204 x 424
12	Clathrin coated pit	VAST	5 x 5 x 5	1 um^3 6 [110 x 110 x 110]	.33 um^3 2 [110 X 110 X 110]
13	Clathrin coated pit	VAST	5 x 5 x 5	1.5 um^3 9 [110 x 110 x 110]	.33 um^3 2 [110 X 110 X 110]
13	ER	GC, VAST	5 x 5 x 5	2.03 um^3 110 x 290 x 510	-
13	Mitochondria	Ilastik, VAST	5 x 5 x 5	1 um^3 200 x 200 x 200	-
13a	Nuclear pore	VAST	5 x 5 x 5	1.33 um^3 8 [110 x 110 x 110]	.33 um^3 2 [110 x 110 x 110]

20	Mitochondria	OpenOrganelle (Heinrich et al., 2021; Xu et al., 2021)	4 x 4 x 3.2	4.51 um^3 500 x 250 x 500 200 x 200 x 200	0.52 um^3 200 x 200 x 200
21	Mitochondria	OpenOrganelle (Heinrich et al., 2021; Xu et al., 2021)	4 x 4 x 3.4	-	1.07 um^3 256 x 256 x 256
22	Mitochondria	OpenOrganelle (Heinrich et al., 2021; Xu et al., 2021)	4 x 4 x 3.4	-	0.22 um^3 150 x 150 x 150
19	ER	OpenOrganelle (Heinrich et al., 2021; Xu et al., 2021)	4 x 4 x 5.2	9.96 um^3 250 x 500 x 500 200 x 200 x 200 250 x 250 x 250 200 x 200 x 200 250 x 400 x 400 238 x 300 x 300	1 um^3 250 x 250 x 250
20	ER	OpenOrganelle (Heinrich et al., 2021; Xu et al., 2021)	4 x 4 x 3.2	4.51 um^3 500 x 250 x 500 200 x 200 x 200	1.07 um^3 256 x 256 x 256
21	ER	OpenOrganelle (Heinrich et al., 2021; Xu et al., 2021)	4 x 4 x 3.4	-	4 um^3 500 x 250 x 500
22	ER	OpenOrganelle (Heinrich et al., 2021; Xu et al., 2021)	4 x 4 x 3.4	-	4.02 um^3 501 x 250 x 502

Description of cells, procedures used to generate ground truths (see methods for details), resolution of FIB-SEM data and size of hold out volumes used for training and validation.

Table S5. Effect of CLAHE on prediction performance of the model

	Mitochondria				Golgi				ER			
Validation blocks in cell	***1***	***2***	***3 naive***	***6 naive***	***1***	***2***	***3 naive***	***6 naive***	***1***	***2***	***3 naive***	***6 naive***
without normaliza-tion	0.98± 0.01	**0.92± 0.02**	0.73± 0.04	0.88± 0.02	0.69± 0.03	0.68± 0.04	0.55± 0.02	**0.80± 0.02**	0.93± 0.01	0.87± 0.04	0.91± 0.01	0.83± 0.02
Linear rescale	0.96± 0.01	**0.92± 0.03**	0.64± 0.07	**0.90± 0.02**	0.68± 0.05	0.71± 0.04	0.51± 0.02	0.74± 0.05	**0.96± 0.01**	**0.92± 0.01**	0.91± 0.01	**0.87± 0.01**
histogram equaliza-tion	0.96± 0.02	0.85± 0.04	0.71± 0.05	0.84± 0.06	0.61± 0.08	**0.74± 0.17**	0.64± 0.06	0.36± 0.10	0.90± 0.02	0.87± 0.03	0.91± 0.02	0.83± 0.03
CLAHE clip 1%	0.97± 0.01	**0.92± 0.02**	0.73± 0.03	0.87± 0.01	**0.70± 0.04**	0.67± 0.03	0.52± 0.02	0.77± 0.03	0.95± 0.01	0.91± 0.01	0.91± 0.01	0.85± 0.01
CLAHE clip 2%	0.96± 0.02	0.87± 0.03	0.75± 0.05	0.88± 0.03	0.56± 0.08	0.69± 0.05	0.56± 0.04	0.79± 0.02	0.95± 0.01	0.89± 0.04	**0.92± 0.01**	0.77± 0.04
CLAHE clip 3%	**0.99± 0.00**	0.89± 0.02	**0.81± 0.03**	0.89± 0.01	0.68± 0.15	0.69± 0.12	**0.66± 0.06**	0.37± 0.25	0.91± 0.02	0.84± 0.06	0.91± 0.02	0.72± 0.05

F1 prediction scores using the indicated cells were obtained with models trained with combined FIB-SEM data from cells 1 and 2 subjected or not to the indicated types of signal normalization. F1 data for each organelle corresponds to the average +/- SD from 20 consecutive predictions obtained every 1000 iterations initiated after about 150,000 training iterations. Best results are highlighted in bold. Inspection of the data shows no consistent improvement in the F1 predictions scores upon signal normalization including CLAHE.

Table S6. Comparative examples of predictive performance by models trained with data from one or two cells

Structure Fixation	F1 for model trained using Cell 1				F1 for model trained using Cell 2				F1 for model trained using Cells 1+2 or Cells 19 + 20			
Cells used for predictions	***1***	***2 naive***	***3 naive***	***6 naive***	***1 naive***	***2***	***3 naive***	***6 naive***	***1***	***2***	***3 naive***	***6 naive***
Mitochondria CF	0.91	0.47	0.66	0.81	0.89	0.87	0.74	0.7	0.96	0.87	0.75	0.88
ER CF	0.86	0.29	0.7	0.52	0.16	0.90	0.83	0.55	0.95	0.90	0.92	0.77
Golgi CF	0.45	0.68	0.61	0.73	0.18	0.62	0.48	0.77	0.56	0.69	0.56	0.79
Cells used for predictions									***19***	***20***	***21 naive***	***22 naive***
Mitochondria HPFS									1	1	0.94	0.93
ER HPFS									0.91	0.80	0.48	0.81

The neural network was trained using ground truths from the indicated cells, alone or in combination, and the resulting models then used to predict from images of the listed individual cells. The data show F1 prediction scores using validation ground truths not employed for training.

Table S7. Comparison of model performance using the ASEM (this study) and COSEM training and prediction pipelines

Source	Structure Fixation	Post Processing	Training Model # Training iterations (x1000)				F1 for the indicated cells used for training		F1 for naive cells		Fine-tuning Training Iterations (x1000)		F1 after fine-tuning	
Cells training and predictions			**19 + 20**				**19**	**20**	**21**	**22**	**21**	**22**	**21**	**22**
this study	Mitochondria HPFS	No	1675 95-115				0.99	0.99	0.94	0.93	2-7	2-7	0.93	0.98
this study	ER HPFS	No	1669 180-200				0.91	0.80	0.48	0.81	7-12	1-6	0.69	0.90
							F1 for the indicated cells used for training							
Cells training and predictions			**19**	**20**	**21**	**22**	**19**	**20**	**21**	**22**				
COSEM	Mitochondria HPFS	Yes	Few 575	All 825	All 875	Many 110	0.93	0.97	0.98	N/A	-	-	-	-
COSEM	ER HPFS	Yes	Many 625	All 1075	Few 625	Many 650	0.84	0.71	0.75	0.97	-	-	-	-

The neural networks used in this study or by the COSEM Project (Heinrich et al., 2021) were trained to predict mitochondria and ER using ground truths from the indicated cells, alone (COSEM Project) or in combination (this study). The data show F1 prediction scores using validation ground truths not employed for training. In this study we only used data from one organelle at a time to train the neural network and report the results for the defined number of training iterations chosen when the performance of the model reached stability; Reported F1 scores are the average of 20 consecutive values obtained every 1,000 training iterations determined after the indicated training iteration. The COSEM project simultaneously used data from more than one organelle to train the neural network according to the details described in (Heinrich et al., 2021). The F1 values for the COSEM Project reported in Tables 1 & 2 (Heinrich et al., 2021) correspond to their best results by different trained networks and training iterations using ground annotations for ‘few’, ‘many’ or ‘all’ organelles including mitochondria and ER present within the holding block.

Table S8. Comparative examples of predictive performance by models trained with data from cells prepared with the same or different fixation protocols

Structure Fixation	Training iterations (x1000)	F1 for model trained using indicated cells	F1 for naive cells	Fine-tuning training iterations (x1000)	F1 after fine-tuning with naive cells
Cells used for training & predictions		***1, 2 (CF)***			
Cells used for predictions			***3, 6 (CF)***		***3, 6 (CF)***
Mitochondria	95-115	0.96 0.87	0.75 0.88	1-6 1-6	0.88 0.89
ER	115-135	0.95 0.90	0.92 0.77	-	-
Golgi	35-55	0.56 0.69	0.56 0.79	-	-
Cells used for training & predictions		***19, 20 (HPFS)***			
Cells used for predictions			***21, 22 (HPFS)***		***21, 22 (HPFS)***
Mitochondria	95-115	0.99 0.99	0.94 0.93	2-7 2-7	0.93 0.98
ER	180-200	0.91 0.80	0.48 0.81	7-12 1-6	0.69 0.90
Cells used for training & predictions		***1,2 (CF)*** ***21, 22 (HPFS)***			
Cells used for predictions			***3,6 (CF)*** ***21, 22 (HPFS)***		***3 ,6 (CF)*** ***21, 22 (HPFS)***
Mitochondria	135-155	0.95 0.81 0.93 0.99	0.73 0.77 0.96 0.89	- 1-6 - -	- 0.90 - -
ER	100-120	0.94 0.90 0.84 0.74	0.85 0.82 0.58 0.81	- - 1-6 -	- - 0.68 -
Cells used for training & predictions		***13a (HPFS)***			

Nuclear pores	130-150	0.52	-		
Cells used for training & predictions		***13 (HPFS)***			
Cells used for predictions			***12 (HPFS)***		
Clathrin-coated pits/ vesicles	80-100	0.67	0.69		

The neural network was trained using ground truths from the indicated cells prepared with different fixation protocols, alone or in combination, and the resulting models then used to predict from images of the individual cells listed in the table. The data show F1 prediction scores using validation ground truths not employed for training.

Table S9. Summary of experiments used to test the effect of fine-tuning

Structure Fixation Protocol	Training cells ground-truth volume [um]	Training iterations (x1000)	Cell F1 prediction	Cell fine-tuning ground-truth volume [um]	Cell Fine-tuning Iterations (x1000)	Cell F1 after fine-tuning
Mitochondria CF	1 + 2 138.2 μm^3	95	3, naïve 0.75 6, naïve 0.88	3, naïve 1.95 μm^3 6, naïve 1.15 μm^3	3, naïve 6 6, naïve 6	3, naïve 0.88 6, naïve 0.89
Mitochondria HPFS	19 + 20 12.12 μm^3	95	21, naïve 0.94 22, naïve 0.93	21, naïve 4.00 μm^3 22, naïve 4.02 μm^3	21, naïve 7 22, naïve 7	21, naïve 0.93 22 0.98
ER HPFS	19 + 20 4.85 μm^3	180	21, naïve 0.48 22, naïve 0.81	21, naïve 1.07 μm^3 22, naïve 0.52 μm^3	21, naïve 12 22, naïve 6	21, naïve 0.69 22, naïve 0.90

Description of models, cells, hold out volumes containing ground truths employed for model training and validation in experiments to test the effect of fine-tuning.